Development of Conductors with Reduced Wind Drag and Wind Noise for Overhead Power Transmission Lines

*by Naoshi Kikuchi *, Yutaka Matsuzaki *2, Hideo Banse *2*
*Takao Kaneko *2, Akihiro Yukino *3 and Hirotaka Ishida *3*

ABSTRACT The wind load acting on the conductors of overhead power transmission lines is a major factor impacting the designed strength of the towers, so that a reduction in wind drag can result in a decrease in construction costs and an improvement in the reliability of the line. The authors have accordingly addressed the problem of reducing conductor wind drag, and propose a reduced-drag design featuring grooves in the conductor surface and a reduced-noise and -drag design featuring grooves and protruding wires. This paper presents a clarification of the mechanism of drag reduction by rendering visible the air flows around the conductors, describes wind tunnel measurements of drag coefficient and field observations of a full-scale test line under high-wind conditions, and the carrying out of a series of tests on basic conductor characteristics and accessories for the completion of a reduced-drag conductor.

1. INTRODUCTION

Designing the strength of the structures that support overhead power transmission lines is significantly influenced by wind drag, and they are designed to withstand the loads bearing on the lines and the support towers themselves (design wind velocity 40 m/sec) imposed primarily during typhoons. When they are situated in a topographical formation such that strong local winds arise as the typhoon passes, the increased wind load is taken into account [1)], and this tends to increase construction costs. The drag on the conductors often accounts for as much as 50-70% of total drag, and any reduction in conductor drag will reduce the load on the support towers, making it possible to reduce costs without compromising reliability.

The authors noted the fact the wind velocity at which the drag coefficient of a cylinder begins to drop is decreased by surface roughness [2)], and the fact that golf balls travel farther because of their dimpled surface [3)], and came to the conclusion that it would be possible to reduce the drag coefficient of a conductor within the range of wind velocities for which transmission lines were designed by focusing their attention on the surface morphology of the conductor. As a result we have proposed conductors with reduced drag, provided with grooves in the surface (the LP 810-mm^2 reduced-drag conductor and the LNP 810-mm^2 reduced-noise and -drag conductor). We also carried out wind tunnel experiments up to a wind velocity of 80 m/sec using full-scale dimensions [4)], clarified the mechanism of drag reduction using a water tunnel [5), 6)], and field observations on a full scale, verifying the aerodynamic characteristics of the reduced-drag conductors.

In addition to the aerodynamic characteristics of the reduced-drag and reduced-noise and -drag conductors, this paper reports tests on basic conductor characteristics and the results of studies on accessories.

2. STRUCTURE OF A CONDUCTOR WITH REDUCED DRAG

Table 1 shows the specifications and cross-section of the 810-mm^2 reduced-drag (LP-810) and reduced-noise and -drag (LNP-810) conductors in comparison with those of a conventional conductor. The outermost layer of the LP-810 (reduced-drag) conductor is a smooth wire, with 12 grooves at equal intervals around the circumference. Similarly the LNP-810 (reduced-noise and -drag) conductor has 12 grooves in the smooth outermost layer and 4-directional protrusions. Since the LP conductors shown in Table 1 are designed to virtually the same current capacity as the conventional conductor, they have slightly smaller equivalent diameters.

3. THE MECHANISM OF DRAG REDUCTION

To reach a clear understanding of the mechanism of drag reduction, a program of visualization of air flow and drag measurement using the water tunnel of the Central

* Engineering Dept., Electric Power Transmission Engineering Div.
*2 Engineering Dept., Bare Wire Div.
*3 The Kansai Electric Power Co., Inc.

Table 1 Characteristics of conductors.

Characteristic	Unit	Specification		
		Conventional TACSR-810	Reduced-drag LP-810	Reduced-noise & -drag LNP-810
Type of conductor		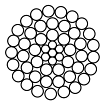	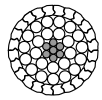	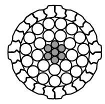
Tensile load	kN {kgf}	180.9 {18,450}	184.1 {18,770}	187.2 {19,090}
Outer diameter	mm	38.4	37.2	Protrusions: 38.8 Declivities: 37.2 Equivalent: 37.9
Calculated cross-sectional area	mm^2	814.5 (TAL)	836.6 (TAL)	858.3 (TAL)
	mm^2	56.29 (ST)	56.29 (ST)	56.29 (ST)
	mm^2	870.8 (Total)	892.9 (Total)	914.6 (Total)
Calculated weight	kg/km	2,700	2,761	2,821
Electrical resistance	Ω/km	0.0363	0.0353	0.0344
Modulus of elasticity	Gpa {kgf/mm²}	71.1 {7,250}	70.9 {7,230}	70.6 {7,200}
Coefficient of linear expansion	/°C	20.8×10^{-6}	20.9×10^{-6}	20.9×10^{-6}
Current capacity	A	1,998 (continuous at 150°C, 60 Hz)	2,003 (continuous at 150°C, 60 Hz)	2,041 (continuous at 150°C, 60 Hz)
		2,007 (continuous at 150°C, 50 Hz)	2,011 (continuous at 150°C, 50 Hz)	2,050 (continuous at 150°C, 50 Hz)

Research Institute of Electric Power Industry, together with oil flow tests using wind tunnel facilities was carried out to obtain information on the nature of flows over the surfaces of LP and LNP conductors.

3.1 Conductors with Reduced Wind Drag

Figure 1 shows a visualization, using a water tunnel, of flows over conductor surfaces. In the case of the conventional conductor, separation occurs approximately 100 deg downstream from the upstream stagnation point, irrespective of wind velocity (Figure 1a). In contrast, it can be confirmed (see Figure 1b) that in the case of the LP conductor, when the drag coefficient is reduced, the separation point of the flow shifts to the downstream side (approximately 120 deg). This represents a rearward shift in self-excited vibration in a free-shear layer (or cavity tone phenomenon), occurring in cavities in the vicinity of 70 deg, by which the after-flow region on the back surface of the conductor becomes smaller and drag is reduced. Even if the conductor is rotated so that the position of the grooves relative to the flow is changed, the same kind of phenomenon occurs confirming that for conductors of this configuration, the position of the grooves has no effect.

3.2 Conductors with Reduced Wind Noise and Wind Drag

When visualized in the water tunnel test, the drag is reduced as the main flow approaches the conductor due to the vortexes generated at the protrusions. At the grooves, in the region where R_e exceeds 7.6×10^4 (wind velocity 30 m/sec) the separation point shifts rearward as a result of a cavity tone in which multiple vibration modes are superimposed. At the same time, due to the overall turbulence occurring toward the rear side, the main stream contacts the conductor and drag is reduced.

In oil flow tests using actual conductors, it was also found that since protrusions and grooves alternate in the conductor axial direction, a forced separation of the flow due to protrusions and a rearward shift in the separation due to the grooves are present alternately along the axis of the conductor.

By these results it was possible to explain the mechanism by which drag was reduced.

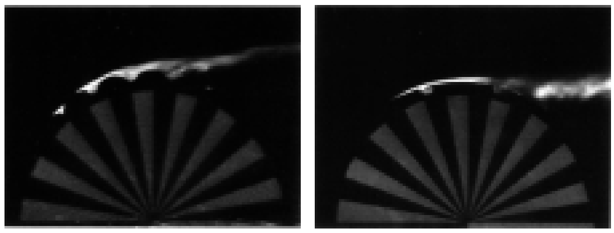

a) Conventional conductor b) Reduced-drag conductor

Figure 1 Visualization of flows over conductor surfaces at point of separation.

4. FEATURES OF CONDUCTORS WITH REDUCED WIND DRAG

4.1 Drag Coefficient

4.1.1 Wind Tunnel Facility

The wind tunnel tests were carried out using three facilities: Research Center for Advanced Science and Technology, University of Tokyo, Canada's National Research Center, and Furukawa Electric.

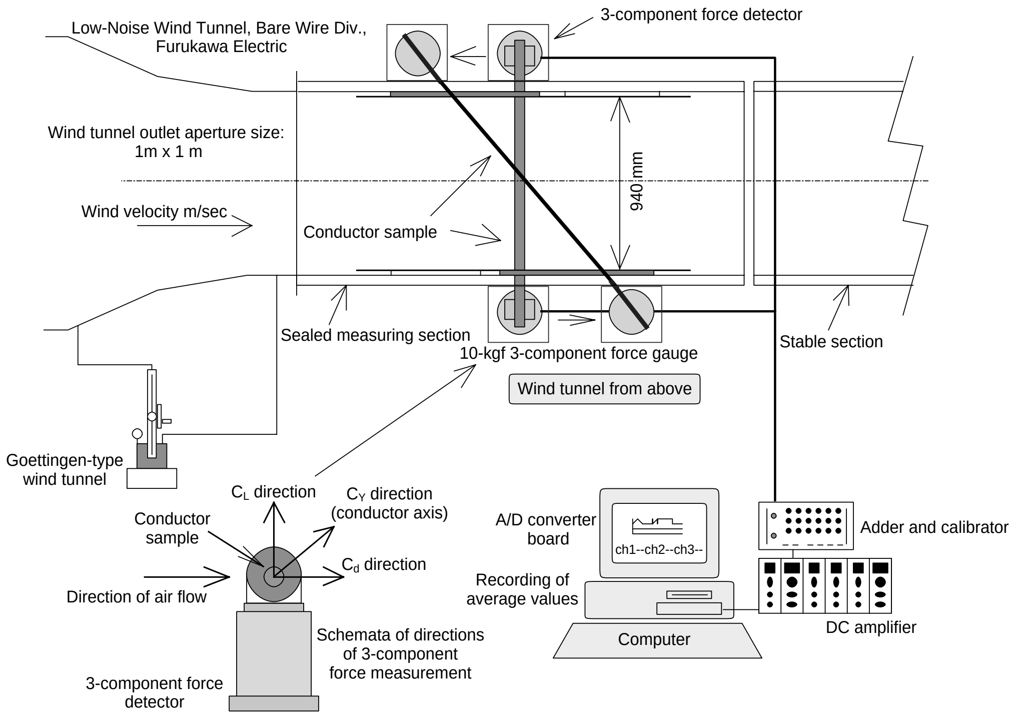

Figure 2 Layout of test equipment in Furukawa Electric's wind tunnel.

The 3-m diameter Goettingen-type wind tunnel at Tokyo University's Research Center for Advanced Science and Technology was used for the investigation of optimum configurations at the onset of the research, and for tests of the aerodynamic characteristics of multi-conductor arrangements for selected prototype reduced-drag configurations. The 2×3-m sealed Goettingen-type wind tunnel at Canada's NRC in Ottawa was used for aerodynamic characteristic tests for single conductors (including incident angles other than 90 deg) up to 80 m/sec. Furukawa Electric's 1×1-m Eiffel type wind tunnel was used for measuring overall aerodynamic coefficients, including such conditions as rain, turbulence, conductor aging, surface fouling and so on. Figure 2 shows the layout of the test equipment in Furukawa Electric's wind tunnel testing facility, in which the measuring section can be either sealed or open, according to the purpose of the test.

A comparison was made between the drag characteristics obtained at the three facilities, and despite differences attributable to the procedures and conditions of measurement a high degree of accuracy was confirmed.

4.1.2 Drag Coefficient When Dry

(1) Conductors with reduced wind drag

Figure 3 shows the relationship between drag coefficient and standard wind velocity at two incident angles (90 deg and 60 deg) for TACSR-810 and LP-810 conductors. At wind velocities from about 25 to 60 m/sec, the LP conductor shows a decrease in drag coefficient of approximately 30% compared to the conventional conductor.

Figure 4 shows the relationship between the incident angle of wind and drag coefficient. The drag coefficient of the LP-810 conductor, like that the TACSR-810 conductor, decreases as $\sin^2\theta$ of the incident angle, so design with respect to oblique winds can be done by the same method as before.

(2) Conductors with reduced wind noise and wind drag

Figure 5 shows the relationship between drag coefficient and standard wind velocity for TACSR-810 and LNP-810 conductors. At wind velocities from 27 about to 40 m/sec, the LNP conductor shows a decrease in drag coefficient of approximately 20% compared to the conventional conductor. Figure 6 shows the relationship between the incident angle of wind and drag coefficient. Although as a result of the protruding filament this conductor has an incident angle vs. drag coefficient curve with a different trend from that of the conventional conductor, it is somewhat lower than that of the conventional conductor even at an angle of 60 deg.

5. FIELD TESTS

To obtain in-the-field verification of the drag-reduction effect in LP conductors, conventional and LP conductors were installed during fiscal 1998 at the Miyakojima Test Line, an actual-scale facility located in Okinawa Prefecture, where typhoons are frequent, and the swing angles of the conductors were compared during the strong winds that accompany the passage of typhoons.

5.1 Description of the Miyakojima Test Line

This test facility is located on the island of Miyakojima approximately 150 m from the shoreline, and consists of three towers and two spans. Although the terrain around the test line is somewhat hilly along the line, it is flat to

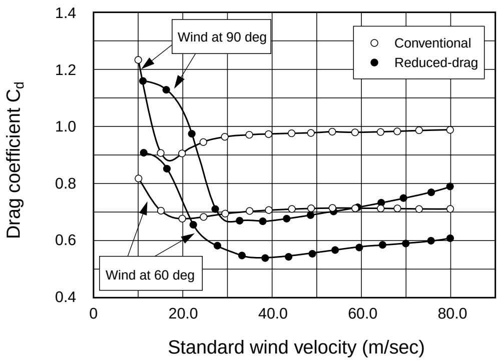

Figure 3 **Drag coefficient vs. standard wind velocity for TACSR-810 and LP-810 conductors.**

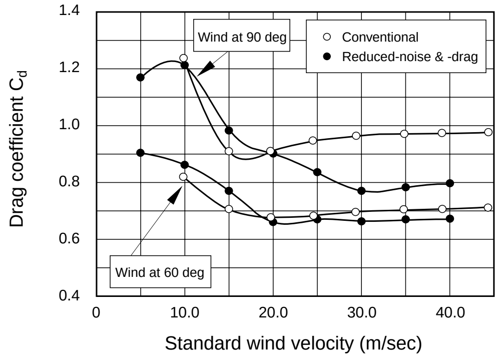

Figure 5 **Drag coefficient vs. standard wind velocity for TACSR-810 and LNP-810 conductors.**

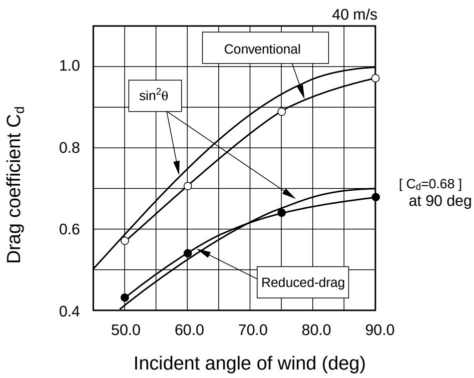

Figure 4 **Incident angle of wind of 40 m/sec vs. drag coefficient for TACSR-810 and LP-810 conductors.**

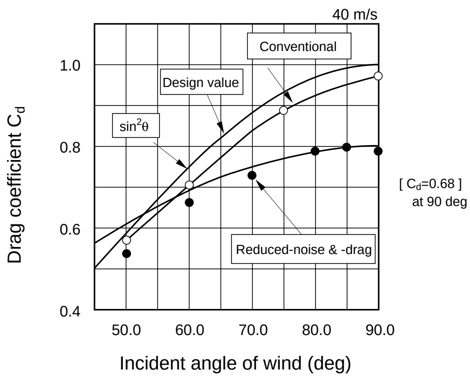

Figure 6 **Incident angle of wind of 40 m/sec vs. drag coefficient for TACSR-810 and LNP-810 conductors.**

both left and right, so that there are no obstacles to crosswinds that might impede measurement for LP conductors. The towers are approximately 25 m in height, and the lowest point of the conductors being measured was 14.2 m above ground (see Figure 7).

Measurements of swing angle were made in the 100-m span between towers #1 and #2. The conventional and LP conductors were strung in parallel with a sag of 5 m, and with no insulators installed.

Generally speaking the static swing angle θ of a transmission line is determined by the mass of the conductor and the wind load and may be stated as:

$$\theta = \tan^{-1}\frac{W_m}{W_c} \qquad (1)$$

where:
θ is the swing angle of a transmission line,
W_m is the wind load on the conductor
(=$1/2 \cdot \rho \cdot V^2 \cdot C_d \cdot D \cdot L$) (kg/m),
where, in turn:
ρ air density (kg·sec²/m⁴),
V is the wind velocity (m/sec),
C_d is the drag coefficient,
D is conductor diameter (m)
L is unit length of conductor (1 m), and
W_c is conductor weight (kg/m)

On the other hand as Figure 8 shows, the displacement of a target attached to the conductor at mid-point in the span was found by processing the images obtained by VCR during high winds, and from this displacement (the observed swing angle,) the swing angle of the conductor under static conditions was calculated geometrically. Wind velocity was measured by a 3-component ultrasonic wind gauge and a vane-type wind gauge mounted atop a 16-m-high concrete tower at the mid-point of the span, data from which were subjected to analog-digital conversion at 0.05-sec intervals and recorded by the computer. The VCR for recording conductor swing was activated whenever wind speed exceeded a set value.

Figure 7 **Miyakojima test line.**

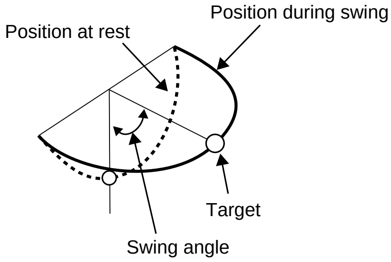

Figure 8 Schematic showing swing angle of conductor.

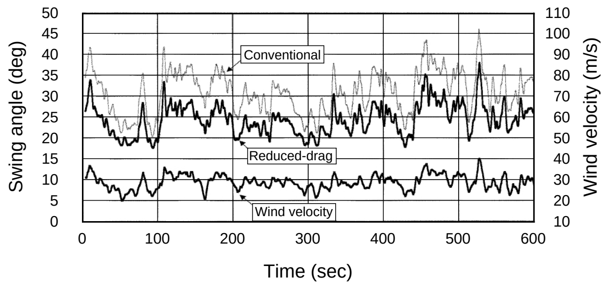

Figure 9 Conductor swing angle vs. wind velocity for TACSR-810 and LP-810 conductors.

5.2 Results of Observations

Figure 9 shows typical time sequence data for wind velocity and the swing angle of the two conductors over a 10-min period during Typhoon 10 in 1998. It can be seen that conductor swing angle closely follows changes in wind velocity.

Figure 10 plots the wind angle against wind velocity using the averages of several 10-min sets of data during the passage of Typhoon 10. Also shown are the curves calculating the respective swing angles taking the drag coefficient of the conventional conductor as 1 and that of the LP conductor as the coefficient curve obtained in wind tunnel experiments. It can be seen that the plotted points for the swing angle of the TACSR are in good agreement with the calculated curve. In the case of the LP conductor, on the other hand, the plot is in good agreement with the calculated curve around 30 m/sec, but at lower wind velocities are below the curve. This is thought to be because, when an LP conductor is placed in a natural wind, the effects of turbulence shift the transitional wind velocity to a lower value than that obtained in wind tests.

Figure 11 plots the 10-min average values of swing angle and wind velocity for TACSR-810 and LNP-810 conductors during the passage of Typhoon 18 of 1999. The 10-min average wind velocity ranged between 15 and 21 m/sec, and the LNP conductor shows good agreement with the curve for swing angle calculated using the drag coefficient obtained in the wind tunnel experiments.

Next, to investigate the response of the LP conductor to wind gusts, the relationship between wind velocity and swing angle was determined for periods of 4 sec, chosen because this represented the period of swing for the conductors strung to this test line, by the following method. Time sequence data on wind velocity and image-processed swing angle (sampling frequency 20 Hz) was

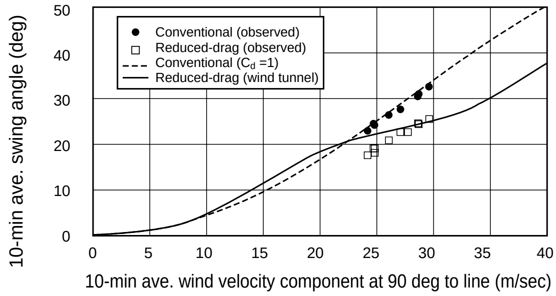

Figure 10 Swing angle vs. wind velocity (10-min ave.) for TACSR-810 and LP-810 conductors.

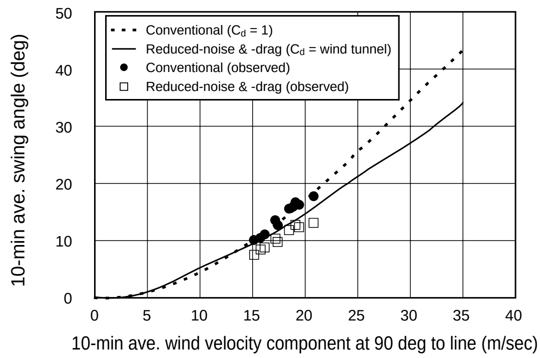

Figure 11 Swing angle vs. wind velocity (10-min ave.) for TACSR-810 and LNP-810 conductors.

divided up at 4-sec intervals producing 80 sets of data which were the averaged, yielding 150 average data for 4-sec periods in 10 min. These data were then segmented using breakpoints every 1 m/sec, the average within each segment was found and wind velocity was plotted against swing angle. Figures 12 and 13 show the results of this processing.

As can be seen from the two figures, the 4-sec ave. wind velocity was from 15 to 40 m/sec, in virtually complete agreement with the curves calculated on the basis of the drag coefficient obtained in the wind tunnel experiments. Thus it was verified that even under typhoon conditions on the field test line, the LP conductor agreed with the drag coefficient measured in the wind tunnel experiments.

6. ENVIRONMENTAL CHARACTERISTIC TESTS

Since the outermost layer of the LP conductor is smooth wire, its wind noise characteristics are inferior to those of the conventional conductor. Accordingly an LNP conductor was developed for use on lines that traverse areas where wind noise is a concern.

Wind noise characteristics were investigated as the environmental characteristics of the LNPconductor. Figure 14 shows the wind noise spectrum in the wind noise test, and it can be seen that noise from the LNP conductor was dramatically lower (10 dB(A) or more) than for the conventional conductor.

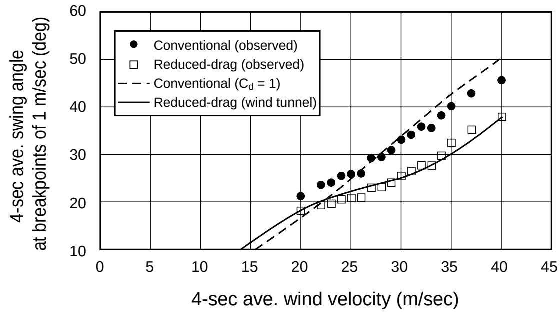

Figure 12 Swing angle vs. wind velocity (4-sec ave.) for TACSR-810 and LP-810 conductors (16 Oct. 1998 21:58-22:08 hrs).

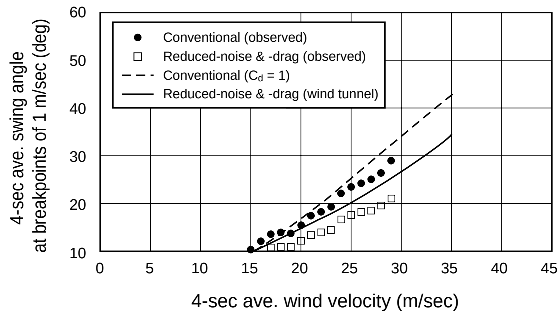

Figure 13 Swing angle vs. wind velocity (4-sec ave.) for TACSR-810 and LNP-810 conductors (21 Sep. 1999, 00:02-00:12 hrs).

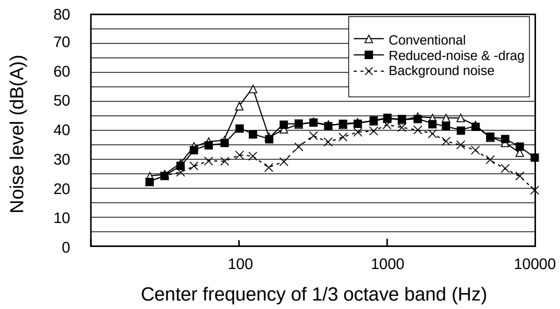

Figure 14 Wind noise for TACSR-810 and LNP-810 conductors (20 m/sec, single conductor).

7. CHARACTERISTICS OF ACCESSORIES

Among the accessories considered for the LP conductor were span-spacers and jumper spacers for multiple conductors, suspension clamps, and dead-end clamps. Thus since the cross-sections of the LP conductor and LNP conductor were either round or nearly round (with a protruding filament that was low), the spacer clamp required no collar or other special structures, and the clamp for the conventional conductor could be adapted by merely changing the diameter of the hole to fit. Similarly the compression-type dead-end clamp and wedge type dead-end clamp can engage by the same method as with the conventional conductor, without the use of collars. It has thus been confirmed that no special structure is required for accessories for the LP conductor, making it superior to the conventional conductor in terms of construction costs.

8. CONCLUSION

We have developed a reduced-drag (LP) conductor having reduced conductor wind load and a reduced-noise and -drag (LNP) conductor combining the two functions of conductor wind load reduction and conductor wind noise reduction, and through a variety of tests have demonstrated its serviceability.

The LP conductor, when used on new power transmission lines, can contribute to savings in construction costs, and when used to replace existing lines will improve reliability with respect to wind load. They have a number of further advantages. If existing lines are replaced with those having the same maximum tension it will, of course, be necessary to consider decreases in vibration fatigue characteristics resulting from increased ordinary tension, but it will be possible to string them with a smaller ordinary sag, thus making it possible to reduce sag and increase capacity. We are confident that they will become widely employed.

In connection with the development of the LP conductor we would like to express our appreciation to the late Mitsuda, professor emeritus, and Masaru Matsumoto, professor, of Kyoto University; to Yozo Fujino, professor of Tokyo University; to Sachio Tamura, professor of Tokyo Institute of Polytechnics; to Yoshirharu Iwatani, professor of Nihon University; and to Hideji Nakamura, associate vice president at The Abiko Research Laboratory and Yuzuru Eguchi, researcher, of the Central Research Institute of Electric Power Industry for their guidance and assistance in research on aerodynamic characteristics; to The Okinawa Electric Power Co., Inc. for their cooperation in field testing; to Asahi Electric Works for their cooperation in research on accessories; and to all others involved.

REFERENCES

1) Japan Electric Association: Research Committee for Electric Technology Standards, Regulations for Overhead Power Transmission, (JEAC 6001-1993) (in Japanese)
2) CHENBACH,E.HEINECKE: On vortex shedding from smooth and rough cylinders in the range of Reynolds number 6×10^3 to 5×10^6, J. Fluid Mech, vol. 109 (1981)
3) Kimura et al.: Flow around a circular cylinder with circular arc grooves on the surface, Visualization Information, Vol.10 Suppl. No.1 (1990-7) (in Japanese)
4) Ishikubo et al.: Study on wind-load reduction of overhead transmission lines, Part III, Conference of Electric Power and Energy Division, IEEJ, No.494, (1997) (in Japanese)
5) Eguchi and Nishihara: Basic study on low wind-load wires -- Investigation on the wind load reduction mechanism of wires through hydrodynamic experiments, Report of CRIEPI, U96516, March 1997 (in Japanese)
6) Eguchi and Nishihara: Basic study on low wind-load wires -- Detailed visualization and theory of the mechanism of wind load reduction, Report of CRIEPI, U97515, March 1998 (in Japanese)
7) Hiratsuka et al.: Results of field tests on low wind-load wires, Part 2, General Conference of IEEJ, No.1623, 1999 (in Japanese)

Manuscript received on November 6, 2001.